ARTICLE
Journal of Cellular Biochemistry 112:2606–2615 (2011)

Journal of Cellular Biochemistry

Tumor Necrosis Factor-α Treatment of HepG2 Cells Mobilizes a Cytoplasmic Pool of ERp57/1,25D$_3$-MARRS to the Nucleus

Brian J. Grindel,[1] Benjamin Rohe,[2] Susan E. Safford,[3] Joseph J. Bennett,[4] and Mary C. Farach-Carson[1*]

[1]*Department of Biochemistry and Cell Biology, Rice University, Houston, Texas*

[2]*Department of Biological Sciences and Center for Translational Cancer Research, University of Delaware, Newark, Delaware*

[3]*Department of Biology at Lincoln University of the Commonwealth of Pennsylvania, Lincoln University, Philadelphia, Pennsylvania*

[4]*Helen F. Graham Cancer Center, Christiana Care Hospital System, Newark, Delaware*

ABSTRACT

ERp57/PDIA3/1,25-MARRS has diverse functions and multiple cellular locations in various cell types. While classically described as an endoplasmic reticulum (ER) resident protein, ERp57 has a nuclear location sequence (NLS) and can enter the nucleus from the cytosol to alter transcription of target genes. Dysregulation and variable expression of ERp57 is associated with a variety of cancers including hepatocellular carcinoma (HCC). We investigated the dynamic mobility of ERp57 in an HCC cell line, HepG2, to better understand the movement and function of the non-ER resident pool of ERp57. Subcellular fractionation indicated ERp57 is highly expressed in the ER with a smaller cytoplasmic pool in HepG2 cells. Utilizing an ERp57 green fluorescent protein fusion construct created with and without a secretory signal sequence, we found that cytoplasmic ERp57 translocated to the nucleus within 15 min after tumor necrosis factor-α (TNF-α) treatment. Protein kinase C activators including 1,25-dihydroxyvitamin D$_3$ and phorbol myristate acetate did not trigger nuclear translocation of ERp57, indicating translocation is PKC independent. To determine if an interaction between the rel homology binding domain in ERp57 and the nuclear factor-κB subunit, p65, occurred after TNF-α treatment and could account for nuclear movement, co-immunoprecipitation was performed under control and conditions that stabilized labile disulfide bonds. No support for a functional interaction between p65 and ERp57 after TNF-α treatment was found in either case. Immunostaining for both ERp57-GFP and p65 after TNF-α treatment indicated that nuclear translocation of these two proteins occurs independently in HepG2 cells. J. Cell. Biochem. 112: 2606–2615, 2011.

KEY WORDS: ERP57; 1,25D3-MARRS; PDIA3; HEPATOCELLULAR CARCINOMA; HEPG2; TNF-α; NUCLEAR TRANSLOCATION; NF-KB

Hepatocellular carcinoma (HCC) is the 5th most common cancer and the third leading cause of cancer related deaths worldwide [El-Serag and Rudolph, 2007]. In the United States, the incidence of HCC and intrahepatic cholangiocarcinoma doubled in the last 30 years [McGlynn et al., 2006], with the 5-year survival rate for individuals with symptomatic HCC only 5% [El-Serag et al., 2001]. The current study examined the expression and potential role of the multifunctional protein disulfide isomerase (PDI) endoplasmic reticulum protein of 57 kDa (ERp57)/PDIA3/GRP58/1,25D$_3$-MARRS in HepG2 cells, a model for HCC. A complex picture exists for ERp57 as both a tumor promoter and a tumor suppressor. During src transformation, expression of ERp57 consistently was upregulated in rat kidney cells [Hirano et al., 1995], a phenomenon it was suggested occurs because it binds and activates STAT3 (signal transducer and activator of transcription) [Eufemi et al., 2004]. Dendritic cells, in contrast, lost ERp57 after exposure to oral squamous cell tumor gangliosides [Tourkova et al., 2005]. Mice exposed to the carcinogen diethylhexyl phthalate lost ERp57 gene and protein expression only in the liver [Muhlenkamp and Gill, 1998]. Similarly, ERp57 protein levels were reduced drastically in gastric cancer and metastases compared to normal gastric mucosa [Leys et al., 2007]. Patients who had lost ERp57 expression in

Grant sponsor: NIH/NIGMS; Grant number: 5SC1GM082365.

*Correspondence to: Dr. M.C. Farach-Carson, Department of Biochemistry and Cell Biology, Rice University, 6100 Main St., Houston, TX 77005. E-mail: farachca@rice.edu

Received 10 May 2011; Accepted 11 May 2011 • DOI 10.1002/jcb.23187 • © 2011 Wiley-Liss, Inc.
Published online 19 May 2011 in Wiley Online Library (wileyonlinelibrary.com).

gastric cancer were less likely to survive after surgery [Leys et al., 2007]. ERp57 has been investigated in primary prostate cancer in its role in the peptide loading complex in MHC class I biogenesis, where its expression, along with other antigen presentation machinery, was reduced in prostate cancer lesions [Seliger et al., 2009]. With respect to resistance to chemotherapy, ERp57 is part of a nuclear multimeric complex including β-actin that is involved in paclitaxel resistance in ovarian cancer [Cicchillitti et al., 2010].

A clue to resolving these complex actions of ERp57 may reside in understanding its dynamic subcellular localization and compartment-specific functions. We investigated the extra-ER localization of ERp57 and the factors that can induce nuclear localization in HepG2 cells. ERp57 is classically viewed as an ER resident protein, where it associates with calnexin and calreticulin to mediate oxidative folding of N-linked glycoproteins [Oliver et al., 1999]. The ER localization is owed to a C-terminal Q/KDEL retention motif, while an N-terminal signal sequence allows initial entry into the ER secretory pathway. However, certain cells demonstrate extra-ER localization. ERp57 is also known as $1,25D_3$-MARRS (membrane associated, rapid response to steroid binding) receptor, that binds the seco-steroid 1,25-dihydroxyvitamn D_3 ($1,25(OH)_2D_3$) and facilitates rapid phosphate and calcium uptake in the duodena of developing chickens and intestinal cells [Ferraro et al., 1999; Nemere, 2005]. Besides the ER and cell surface localization that is consistent with the protein's signal sequence, ERp57 also is localized in the cytosol, inner nuclear matrix, and nucleus of cells [Hirano et al., 1995; Guo et al., 2002]. A weak signal sequence may contribute to this phenomenon in conjunction with a nuclear signal sequence (NLS) present in ERp57 [Shaffer et al., 2005; Adikesavan et al., 2008]. In comparison to binding protein (BiP), an ER resident chaperone protein, ERp57's signal sequence has a destabilizing proline in the alpha helical region that may contribute inefficient binding of the signal recognition particle (SRP) and a subsequent cytoplasmic pool of ERp57. This potentially frees a cytoplasmic fraction of ERp57 to translocate to the nucleus. ERp57 associated with scaffold/matrix associated region (S/MAR)-like sequences of DNA [Coppari et al., 2002], and in melanoma M14 cells, ERp57 associated with STAT3 in the nucleus [Eufemi et al., 2004]. ERp57 was required to associate with Ref-1 in the nucleus to reductively activate the transcription factor AP-1, allowing it to bind its DNA promoter sequence [Grillo et al., 2006]. When DNA binding targets of ERp57 in HeLa cells were cloned, ERp57 was found to bind gene expression regulatory regions, including for stress response genes [Chichiarelli et al., 2007]. All of these data indicate that ERp57 has unidentified functions in the nucleus, likely having pleiotropic effects on gene expression. By extension, dysregulation of ERp57 signaling in the nucleus may contribute to HCC.

ERp57 has a Rel homology binding domain [Khanal and Nemere, 2007]; therefore, NF-κB could provide a carrier shuttle for ERp57 nuclear translocation. It was shown recently that ERp57 can associate with the transcription factor nuclear factor κB (NF-κB) in NB4 promyelocytic leukemia cells [Wu et al., 2010]. Specifically, the p65 subunit (RelA) of the active NF-κB heterodimer binds ERp57 in these cells. Both ERp57 and NF-κB translocated to the nucleus after treatment with a PKC activator phorbol 12-myristate 13-acetate (PMA) or $1,25(OH)_2$ D_3 preceding differentiation of NB4 leukemia cells [Wu et al., 2010].

NF-κB is both higher in expression and more localized to the nucleus in HCC than surrounding tissues [Zhou et al., 2009]. In addition, tumor necrosis factor-α (TNF-α), a potent activator of NF-κB, has higher expression in HCC tissues [Zhou et al., 2009]. This study aimed to find conditions conducive to translocation of ERp57 into the nucleus of HepG2 cells. Specifically, we tested if TNF-α, PMA, or $1,25(OH)_2D_3$ triggered ERp57 nuclear translocation. Additionally, we determined if a fraction of ERp57 is in the cytosol of HepG2 cells where it can translocate into the nucleus during dynamic cell signaling such as might occur in HCC.

MATERIALS AND METHODS

CELL CULTURE

HCC cells, line HepG2, were obtained from American Type Culture Collection (Manassas, VA). Cells were maintained in Gibco's Dulbecco's modified Eagle's medium (DMEM) (Invitrogen, Carlsbad, CA) supplemented with 10% (v/v) heat inactivated fetal bovine serum (FBS) (Invitrogen) and 1% (v/v) penicillin/streptomycin (Invitrogen). The cells were grown in a 37°C incubator with 5% (v/v) CO_2, and passaged at 90% confluency with 0.25% (w/v) trypsin–EDTA (Invitrogen).

PLASMID DESCRIPTION AND TRANSFECTION

DNA plasmids were designed off a mammalian expression vector from Clontech (Mountain View, CA). The endoplasmic reticulum-monomeric red fluorescent protein (ER-mRFP) plasmid was an mRFP with an N-terminal prolactin signal sequence and C-terminal KDEL ER retention sequence. The ERp57-GFP plasmid encoded the human ERp57 protein with its natural signal sequence and a C-terminal GFP containing an A206K mutation, followed by a KDEL ER retention sequence. Both plasmids have a constitutive promoter and a kanamycin and neomycin resistance cassette for selection. CytoERp57 plasmid was developed by utilizing Stratagene's (Santa Clara, CA) site directed mutagenesis kit to remove the start methionine from ERp57-GFP and placing it after the signal sequence. All plasmids were amplified using DH5α competent bacterial cells (Invitrogen) and Qiagen's Maxi-prep kit (Valencia, CA).

All DNA plasmids (ER-mRFP, ERp57-GFP, cytoERp57-GFP) were transfected into HepG2 cells using Lipofectamine 2000 Reagent (Invitrogen) in a 4 μg/10 μl of DNA to Lipo2000 ratio, according to the manufacturer's directions. Reagent and DNA use was scaled according to well size and manufacturer's recommendations. Three-lakh cells/well were seeded into a 6-well plate in 10% FBS DMEM (normal culturing medium) and allowed to reach 90% confluency. FBS DMEM was removed from cells and replaced with serum free (SF) DMEM for 24 h. Four micrograms of DNA was added to 250 μl of OptiMEM (Invitrogen), and 10 μl of Lipo2000 was added to a separate tube containing 250 μl of OptiMEM. Solutions were incubated 5 min at room temperature (RT). The DNA and Lipo2000 OptiMEM solutions were mixed together and incubated for 25 min at RT. The SF DMEM was removed from HepG2 cells and replaced with 2 ml of OptiMEM and the incubated DNA/Lipo2000 solution was

added. After the 6 h incubation at 37°C and 5% CO_2, the cells were washed briefly in PBS and 10% FBS DMEM was added. Forty-two hours later, or 48 h post-transfection, cells either were treated in an experiment or selected against using G418. To generate stable transfectants, 48 h post-transfection, the medium was replaced with 1 mg/ml of G418 sulfate (Geneticin from Invitrogen) in 10% FBS DMEM, and changed every 48 h. Colonies were selected after 14 days, seeded into a 96-well plate, then a 24-well plate, and then a 6-well plate. Selected colonies expanded into flasks were maintained in 500 μg/ml G418. Prior to treatments of stable transfectants, cells were removed from G418 to reduce any potential antibiotics effects.

TREATING HepG2 CELLS WITH TNF-α, H_2O_2, 1,25(OH)$_2$D$_3$, AND PMA

PMA (cat# PE-160) and 1,25(OH)$_2$D$_3$ (cat# DM-200) were obtained from Biomol (Plymouth Meeting, PA). Human TNF-α was obtained from Roche Diagnostics (Basel, Switzerland) (cat# 11-371-853-001) and H_2O_2 was obtained from Fisher (cat# H325-500). HepG2 cells were treated with PMA, 1,25(OH)$_2$D$_3$, and DMSO vehicle control in combinations indicated in the results. Cells were incubated at varying times in a tissue culture incubator at 37°C in 5% CO_2. Following treatment, the media was removed, the cells washed with PBS, fixed for 15 min in 4% (v/v) paraformaldehyde (EMS, Hatfield, PA) in PBS, washed with PBS and viewed under the confocal microscope in PBS no more than 1 day after treatment. Cells were treated with varying combinations of TNF-α, H_2O_2, and BSA vehicle control as indicated in the Results Section and incubated for varying times in a culture incubator at 37°C in 5% CO_2.

STAINING CELLS FOR NF-κB AND NUCLEUS FOLLOWING TNF-α AND H_2O_2 TREATMENT

Stably or transiently transfected HepG2 cells were visualized in wells of a two or eight chambered Lab-Tek II Chamber #1.5 German Coverglass System (Nunc, Rochester, NY) for viewing under an inverted confocal microscope. Following treatment, HepG2 cells were rinsed twice with PBS, and then incubated for 15 min at RT with 4% (v/v) paraformaldehyde in PBS (pH 7.4). The cells were washed again with PBS followed by a 10 min incubation at RT in 0.1% (v/v) TritonX-100 (Fisher, BP151-100) in PBS. Following a brief wash in PBS, the cells were blocked in 3% (w/v) BSA in PBS for 45 min at RT. The blocking solution was removed and replaced with 1:200 NF-κB (p65(A)) rabbit polyclonal primary antibody (Ab) (SantaCruz Biotech, Santa Cruz, CA, cat# SC-109) in 3% BSA in PBS overnight (O/N) (16–18 h) at 4°C in the dark. Peptide blocks were performed to ensure Ab specificity. One microliter of NF-κB Ab and 10 μl of NF-κB (p65(A)) peptide block (SantaCruz Biotech, cat# SC-109P) or 10 μl of peptide block alone were added to 100 μl 3% BSA in PBS and incubated for 1 h at RT. These solutions were added to separate wells containing HepG2 cells for the same time and conditions as the primary Ab alone. Following O/N incubation, cells were washed for 10 min three times (3 × 10 min) in PBS. A 1:200 dilution of 2 mg/ml AlexaFluor 568 conjugated goat anti-rabbit secondary Ab (Invitrogen, cat# A11036) and 1:3,000 dilution of Draq5 (Biostatus, Leicestershire, England) in PBS was prepared and incubated with the cells for 45 min at RT in the dark. The cells then were washed 3 × 10 min with PBS and viewed under a Zeiss LSM 510 VIS confocal microscope attached to an Axiovert 100 M. A 100× Plan-Apochromat (NA (numerical aperature) 1.4) oil immersion and 63× Plan-Aprochromat (NA 1.2) oil immersion objective was utilized. Fluorescence imaging was achieved using an ArKr laser for 488 nm (green, ERp57-GFP) and 568 nm (red, NF-κB Ab) excitation and a HeNe laser for 633 nm (blue, Draq5 nuclear stain) excitation.

CO-IP OF NF-κB AND ERp57 IN HepG2 CELLS FOLLOWING TREATMENT

Protein G agarose (KPL, Gaithersburg, MD) was blocked previously using the following protocol and up- or down-scaled proportionately depending on the amount of agarose needed. Protein G agarose was transferred to a 15 ml conical tube and centrifuged at 1,000*g* for 4 min. The supernatant was discarded, 2.2 volumes of FBS was added to the remaining agarose pellet, and the solution was incubated O/N at 4°C on an end-over-end nutator. Four minutes centrifugation at 1,000*g* followed to pellet resin. The supernatant was discarded and washed three times with 3.5 volumes PBS, centrifuged at 1,000*g* and the supernatant discarded in between. Next, 1.5 volumes of 0.1 M Na citrate, pH 3.5, was added and incubated for 2 min. Tris (1 M), pH 8.0, was added at an 8:5 citrate/Tris ratio, and the solution was centrifuged for 4 min at 1,000*g*, discarding the supernatant thereafter. The resin was washed again as before four times with 3.5 volumes of PBS. The agarose resin was resuspended to 50% (v/v) slurry with PBS and stored at 4°C.

Several variations of the co-IP protocol described here are specified in the Results Section as they relate to individual experiments. After treatment, the medium was removed from HepG2 cells in 6-well plates and washed briefly with PBS. To the cells, 1 ml of 50 mM *N*-ethylmaleimide (NEM) (Pierce, prod# 23030) in cold PBS was added, and placed on ice for 5 min. The 50 mM NEM PBS solution was removed and 0.75 ml cold 0.5% (v/v) Nonidet P40 (NP40) (Roche, cat# 11-754-599-001) in PBS with 10 mM NEM, 1/100 protease inhibitor cocktail (PIC) (Sigma, cat# P8340), and 1/100 phosphatase inhibitor cocktail (Calbiochem, Madison, WI, cat# 524625) was added, the cells were then scraped loose with a cell scraper, and incubated on ice for 20 min. Lysates for each time point or condition (e.g., 15 min TNF-α or vehicle control treatment) were collected in a microcentrifuge tube and centrifuged at 10,000*g* at 4°C for 15 min to pellet any cell debris. The supernatant was equally divided into separate centrifuge tubes: one for incubation in 2 μg/ml non-immune ChromPur Rabbit IgG (Jackson ImmunoResearch, cat# 011-000-003), one for incubation in 2 μg/ml p65 (NF-κB) Ab (SantaCruz Biotech, SC-109), and, in some experiments, one for incubation with 2 μg/ml of a rabbit polyclonal Ab specific for the C-terminus of ERp57 (Affinity BioReagents, cat# PA3-009). After adding the appropriate amount of Ab to the HepG2 lysate (425 μl), the combination was incubated O/N at 4°C on a nutator. One hundred microliters of pre-blocked Protein G agarose was added to the 425 μl of the Ab-incubated lysate, and placed on a 4°C nutator for 5 h. The solution was centrifuged at 10,000*g* for 4 min at 4°C, and the supernatant discarded (some was collected for analysis). The Ab–resin–protein complex was washed twice with 0.5% NP-40 and 10 mM NEM in PBS, where it was centrifuged at 10,000*g* in between, discarding the wash supernatant. The pellet was washed three times in 10 mM NEM in PBS, centrifuged at 10,000*g* in between,

discarding the wash supernatant. After the final supernatant was removed, 40 μl of Laemmli sample buffer (LSB) (Bio-Rad, Hercules, CA) with 5% (v/v) β-2-mercaptoethanol and 40 μl sample extraction buffer (SEB) (0.5 M Tris pH 6.8, 8 M urea, 1% (w/v) SDS (sodium dodecyl sulfate), 0.01% (w/v) phenylmethyl sulfonylfluoride, 1% (v/v) β-mercaptoethanol in Barnstead water) was added to the resin, vortexed, boiled for 3 min, vortexed again, and centrifuged at 10,000*g* at RT for 1 min. An equal volume (25 μl) of each remaining supernatant was loaded into every lane for examination after gel electrophoresis.

HepG2 SUBCELLULAR FRACTIONATION THROUGH DIFFERENTIAL CENTRIFUGATION

HepG2 cells were grown to confluency in 10% FBS DMEM in T75 flasks. The medium was removed, the cells washed twice with PBS, and then incubated in a tissue culture incubator (37°C, 5% CO_2) for 35 min in 10 mM EDTA in PBS to detach cells. Cells were centrifuged at 500*g* for 5 min, the supernatant removed, and resuspended in homogenization buffer (0.25 M sucrose, 5 mM HEPES (4-(2-hydroxyethyl)-1-piperazineethanesulfonic acid), 1:100 PICs, pH 7.4, cold). The cells were homogenized gently on ice with 10 strokes of a loose B type pestle (Wheaton Science, Millville, NJ). For analysis, 1 ml of homogenate was collected. Homogenates were transferred to Corex tubes, then placed in a Sorvall RC-5B Refrigerated Superspeed Centrifuge, and centrifuged at 6,000*g* for 8 min at 4°C using an SS-34 rotor. The supernatant was collected, and the pellet resuspended in homogenization buffer (sample fraction P6). The supernatants were moved to polyallomer tubes, placed in a Beckman L855M Ultracentrifuge with an SW41-Ti rotor, and centrifuged at 105,000*g* at 4°C for 45 min. The supernatant (cytoplasmic fraction, S105) was collected, and the pellet was resuspended in homogenization buffer (microsomal fraction, P105).

GEL ELECTROPHORESIS, WESTERN TRANSFER, AND WESTERN BLOT

Following standard trichloroacetic acid protein precipitation and standard Lowry protein assay, protein samples were separated using sodium dodecyl sulfate–polyacrylamide gel electrophoresis (SDS–PAGE) with a 15% Porzio and Pearson resolving and a 4.5% stacking gel. Samples were mixed with reducing LSB, boiled in a water bath for 2 min, and loaded into gel lanes according to μg of protein (for differential centrifugation). Proteins were separated by electrophoresis at constant voltage (130 V) in running buffer (0.05 M Tris base, 0.15 M glycine, 0.1% SDS), then transferred to a nitrocellulose membrane with constant voltage (40 V) at 4°C for 5 h in transfer buffer (0.1 M Tris base, 0.1 M glycine). Transferred proteins were examined by western blot, where the protocol varied for the protein of interest. For ERp57, the membrane was blocked with 5% (w/v) Carnation brand non-fat dry milk in PBST20 O/N (12–15 h) on a shaker at 4°C. Ab to ERp57 (Affinity BioReagents, rabbit polyclonal) was added directly to blocking solution at a 1:2,500 dilution and incubated for 2 h on a shaker at 4°C. The membrane was washed 3 × 5 min with PBST20, and incubated with 1:200,000 HRP-conjugated goat anti-rabbit secondary Ab (Pierce, 10 μg/ml, prod# 1858415) in 3% BSA in PBST20 for 2 h on a shaker at 4°C. Following a 3 × 5 min PBST20 wash on a shaker, the membrane was placed in Super Signal West Dura Extended Substrate (Pierce, prod# 34076) for 5 min at RT and exposed. For β-actin, the protocol was the same as ERp57 but following the block the membrane was washed briefly in PBST20, and replaced with 1:5,000 β-actin rabbit polyclonal Ab (Abcam, Cambridge, MA, code ab8227-50) in 3% BSA in PBST20, and incubated O/N on a shaker at 4°C. For BiP (binding protein) the procedure was the same as ERp57 except the membrane was removed from the milk block, briefly washed in PBST20, and incubated with 1:2,000 rabbit polyclonal Ab to BiP (Abcam, code ab21685) in 3% BSA in PBST20 O/N on a shaker at 4°C. Developed film was viewed under a Multi-Image Light Cabinet (Alpha-Innotech Corp.) and captured with Alpha-Imager software.

RESULTS

CONSTRUCTS

Several protein fusion constructs were designed to track the dynamic movements of the separate pools of ERp57 and are shown in Figure 1. Panel A shows a monomeric red fluorescent protein (mRFP) with a strong prolactin signal sequence (a highly secreted protein) [Shaffer et al., 2005] and a KDEL ER retention sequence that created a strong reference RFP signal in the ER. Panel B shows ERp57 that was cloned with a green fluorescent protein tagged to the C-terminus followed by a KDEL ER retention sequence, thus ensuring retrieval of ERp57 into the ER rather than it being secreted into the extracellular space. The construct in Panel B retains the protein's native N-terminal signal sequence, therefore, partitions between the ER and the cytosol based on the strength of the signal sequence. In this case, any non-ER localization was due to inefficient ER translocation of the SRP complex. In Panel C, a fully cytoplasmic ERp57-GFP (cytoERp57-GFP) is shown. To create this, the ERp57 signal sequence was removed, leaving the protein unable to find the SRP and therefore unlikely to enter the ER.

ERp57 SUBCELLULAR LOCALIZATION IN HepG2 CELLS CO-TRANSFECTED WITH ERp57-GFP AND RFP AND DURING CELL FRACTIONATION

To assess the subcellular distribution of ERp57, HepG2 cells were co-transfected with ERp57-GFP (from Fig. 1, panel B) and mRFP (from Fig. 1, panel A) plasmid constructs and viewed live 48 h later under a confocal microscope (Fig. 2). Localization of ERp57-GFP in the ER produces a yellow ER (red mRFP and green ERp57-GFP combined). Any ERp57-GFP outside the ER appears as green signal alone. A live HepG2 cell transiently transfected with both ERp57-GFP and mRFP is shown in Figure 2, panel A. The ER system visualized by this method (yellow) was highly developed in HepG2 cells, occupying a large majority of cellular space. This was expected because parenchymal liver cells have a highly developed ER network for secretion. ERp57-GFP was strongly co-localized with mRFP in the ER, showing no clearly visible evidence of diffuse green staining such as would be seen if there was a large cytoplasmic pool of ERp57. Nuclei are dark. Note, however, round inclusions containing ERp57-GFP that were found in some cells (white arrow in Fig. 2, panel A). Figure 2, panel B shows an enlarged image of these inclusion-like structures. Together, tagged protein expression and imaging suggest that in untreated HepG2 cells, ERp57-GFP is largely

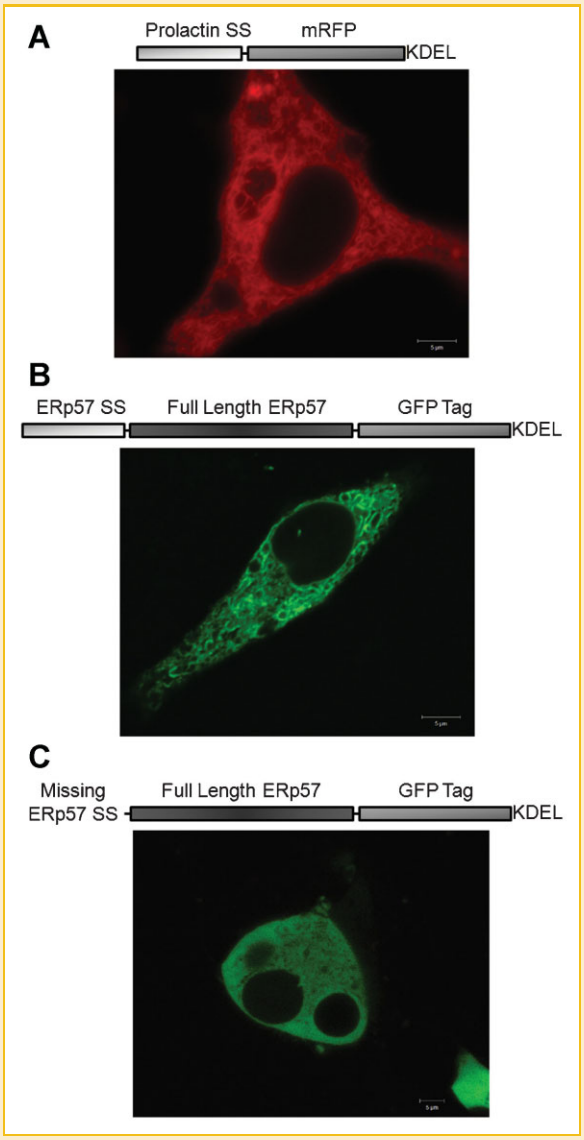

Fig. 1. Proteins expressed off plasmid constructs. A: The ER-mRFP construct encodes a monomeric red fluorescent protein (mRFP) preceded by a prolactin signal sequence and ending in a KDEL ER retention sequence for strong localization to the ER. The mRFP signal image below displays the ER-mRFP localization indicative of HepG2 cells. B: The ERp57-GFP construct encodes full length ERp57 with its natural signal sequence followed by a green fluorescent protein (GFP) and a KDEL ER retention sequence. The GFP signal image below shows the usual ERp57-GFP localization in HepG2 cells. C: The CytoERp57-GFP construct is the same as ERp57-GFP except it does not have a signal sequence. This lack of signal sequence results in ERp57 being diffusely expressed in the cytosol of HepG2 cells as seen in the bottom image.

confined to the extensive ER network in these cells, with strong extra-ER expression in unidentified inclusion-like structures.

Because the intense expression of ER-localized ERp57-GFP will obscure a smaller pool of cytoplasmic ERp57-GFP, subcellular fractionation was performed to separate intact ER from the cytosol. Subcellular fractionation of HepG2 cells was achieved through differential centrifugation. Presented in Figure 2C–E are separated proteins from a flask of cells differentially centrifuged and subjected to Western blot analysis for ERp57, BiP/GRP58, or β-actin. Differential centrifugation produced four fractions: homogenate (H), pellet debris after 6,000*g* spin (P6), microsomal pellet containing ER after 105,000*g* spin (P105), and cytoplasmic fraction from resulting supernatant after 105,000*g* spin (S105). ERp57 (2E) was highly expressed in the H, P6, and P105 fractions. This demonstrated that ERp57 is well expressed in the HepG2 cells and the vast majority is highly localized to the ER. A very faint band of ERp57 is detected in the HepG2 cytoplasmic fraction, S105 (boxed). BiP (2D) a protein highly localized to the ER shows a similar pattern as ERp57. BiP (the two protein bands, arrows) was expressed in HepG2 cells and also was present in the microsomal fraction. BiP had a very small presence in the cytoplasmic fraction. β-actin (2C), a protein localized to the cytosol, was highly enriched in the cytoplasmic fraction and reduced considerably in the microsomal fraction, confirming the cytosol was being separated from the microsomal fraction in these protocols. A strong signal was seen in the S105 fraction, as expected. To further corroborate these findings, a modified differential centrifugation procedure utilizing a different number of strokes and centrifugation times produced similar western blot results (not shown). Therefore, although confocal images of fluorescent cells did not reveal a clear cytoplasmic fraction of ERp57, once intact ER was removed by cellular fractionation, the presence of a small pool of cytoplasmic ERp57 was observed.

ERp57 LOCALIZATION AFTER TREATMENTS WITH PMA, $1,25(OH)_2D_3$, AND TNF-α

HepG2 cells transfected with ERp57-GFP or cytoERp57-GFP were treated under various conditions and for various times to study their potential for nuclear translocation. Following transient transfection of HepG2 cells with the ERp57-GFP plasmid, cells were treated with 100 or 200 nM PMA, a PKC activator, or 10 or 20 nM $1,25(OH)_2D_3$ for 15 min or 1 h. No differences between the vehicle (0.02% dimethyl sulfoxide in SF DMEM) and any of the treatment conditions were observed (results not shown). In contrast, Figure 3 displays the results after treating ERp57-GFP transiently transfected HepG2 cells with 30 ng/ml TNF-α or vehicle BSA treatment for 15 min or 1 h. Following treatment, cells were fixed, permeabilized, and double stained for NF-κB using a p65 Ab (visualized as red) and nuclei with Draq5 (visualized as blue). Cells were stained for p65 to monitor NF-κB's nuclear translocation. p65 Ab controls using blocking peptides incubated with the primary Ab were included to demonstrate Ab specificity. Figure 3A shows a representative 1 h vehicle control treatment, and results were the same for the 15 min vehicle control (not shown). Neither p65 nor ERp57-GFP showed nuclear staining in control cells. Treatments with TNF-α for 15 min (Fig. 3B,D) produced a marked relocation of ERp57-GFP into the nucleus. Using a two-sample test for equality of proportions, there was a statistically significant difference between the proportion of nuclear ERp57-GFP in control (3/56) and treated (18/52) (z-value = 12.92, *P*-value = 0.0003). Meanwhile, the one hr TNF-α treatments (Fig. 3C) produced no noticeable difference in the localization of ERp57-GFP. Figure 3D shows the specificity of the NF-κB Ab through a negative control blocking peptide. Important to mention is that not every transfected cell showed ERp57-GFP nuclear

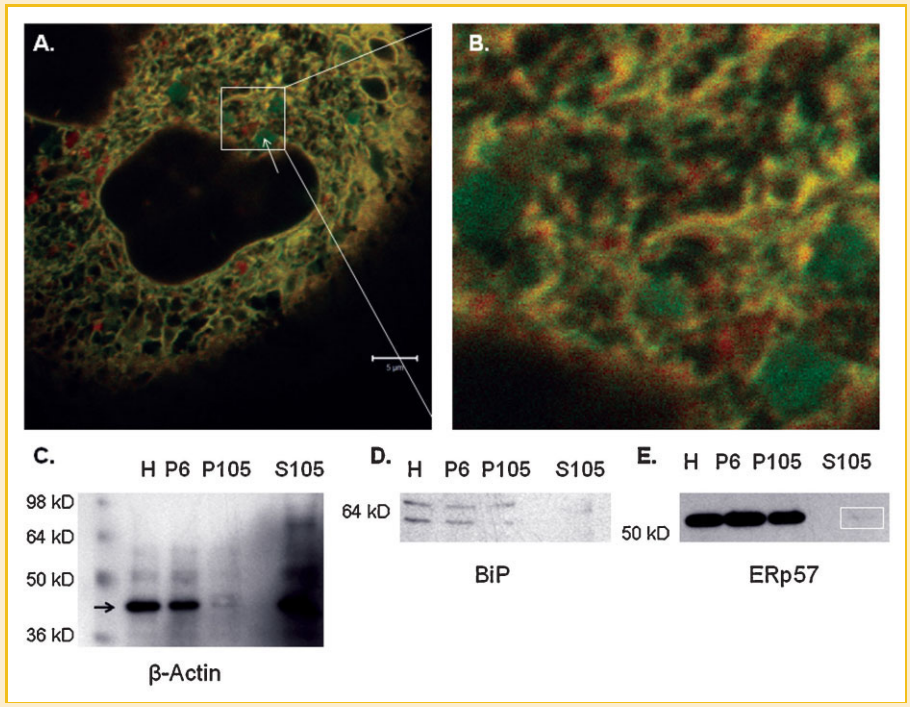

Fig. 2. ERp57 is highly expressed in HepG2 ER relative to cytoplasmic fractions. A,B: Transiently transfected ERp57-GFP was highly co-localized with mRFP in the ER. Obvious green round structures were visible in some cells (white arrow 2A). Images at 100× objective, 2× zoom. C–E: Shown are the Western blots for β-actin, BiP, and ERp57 of differentially centrifugated HepG2 cell fractions. The Materials and Methods section describes the differential centrifugation procedure and the text describes the results. H: homogenate; P6: resuspended pellet after 6,000*g* spin; P105: resuspended pellet after 105,000*g* spin (microsomal fraction); S105: supernatant after 105,000*g* spin (cytoplasmic fraction).

localization after 15 min TNF-α treatments. In summary, treatment of HepG2 cells for 15 min with TNF-α induced nuclear localization of ERp57-GFP in transfected cells, while neither PKA activation nor the steroid $1,25(OH)_2D_3$ triggered translocation under similar treatment conditions.

To determine if the cytoplasmic portion of ERp57 can translocate to the nucleus in HCC cells, HepG2 cells were transfected with cytoERp57-GFP (see Fig. 1C). TNF-α (30 ng/ml) treatment for 15 min increased the number of cells showing nuclear cytoERp57-GFP (Fig. 4B) over vehicle control (Fig. 4A). Also noted is that cytoERp57-GFP showed some steady-state nuclear localization without treatment. Nonetheless, in comparison to control cells (12/76), the treated cells had significantly more cytoERp57-GFP nuclear presence (52/119) (z-value = 15.14, *P*-value = 0.0001). The p65/NF-κB red signal had a greater presence in the nuclei of treated versus untreated cells. Interestingly, movement of p65 after treatment with TNF-α did not depend upon cytoERp57-GFP for nuclear translocation, nor did cytoERp57-GFP nuclear movement depend upon p65. Figure 4B clearly shows red p65 nuclear signal without cytoERp57-GFP nuclear localization (example shown with solid white arrow), and green cytoERp57-GFP nuclear localization without p65 nuclear localization (example shown with dashed white arrow). Therefore, the cytoplasmic fraction of ERp57-GFP can translocate to the nucleus after 15 min of treatment with TNF-α, a phenomenon that can occur independently from NF-κB p65 nuclear translocation.

To further determine if p65 complexes with ERp57 for nuclear translocation in HepG2 cells, a co-IP study was performed after treatment with TNF-α. Figure 5 displays one illustrative variation of this study and the resulting Western blot for p65 and ERp57. Proteins from HepG2 cells treated with BSA vehicle control or 30 ng/ml TNF-α for 15 min were immunoprecipitated using protein G agarose and p65 Ab (Fig. 5, lane B) or control IgG (Fig. 5, lane C). The Western blot for p65 demonstrates the immunoprecipitation was specific for p65 (Fig. 5, WB p65, black arrow). The protein also is detectable in the whole cell lysate lane, but in much lower quantities than the enriched p65 IP lane (Fig. 5, lane A). The western blot for ERp57 clearly shows strong signal in the whole cell lysate (lane A, black arrow), but no signal is detected in the p65 Ab IP lane (lane B) for either the vehicle or TNF-α treated cells. This experiment was repeated with NEM in the lysis buffer as a disulfide stabilizing agent and using different time conditions (30, 60 min), and the same results were observed (not shown). Additionally, a variety of treatments and subsequent co-IPs with ERp57 antibodies recognizing both ends of the protein did not produce a detectable p65 protein band under any condition (not shown). Together, all of these data indicate that endogenous ERp57 and the p65 subunit of the NF-κB do not form stable high affinity complexes either alone or after TNF-α treatment in HepG2 cells.

DISCUSSION

ERp57 SUBCELLULAR DISTRIBUTION IN HepG2 CELLS

ERp57 has multiple demonstrated functions. These activities, ranging from vitamin D steroid responsiveness to transcription

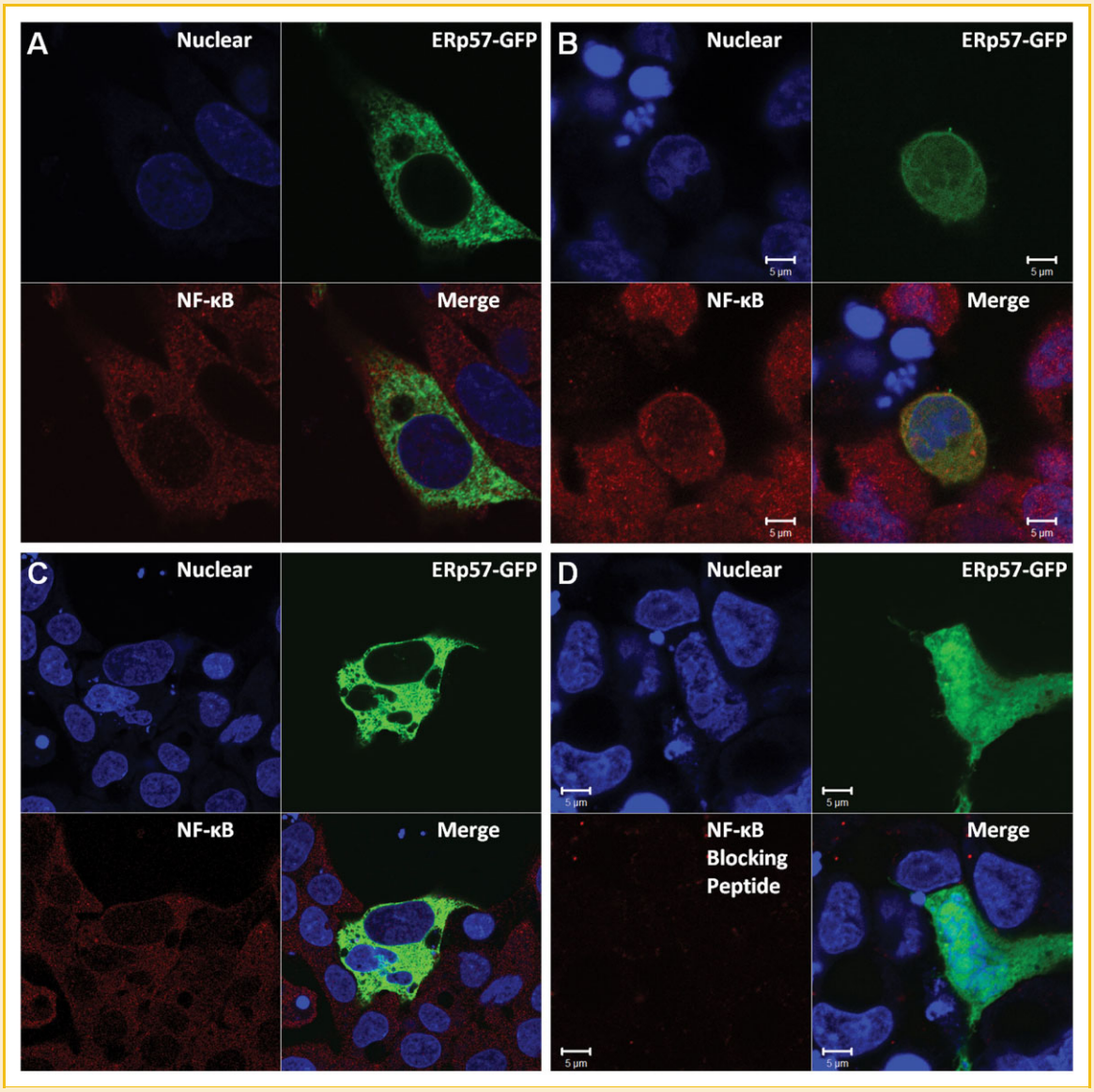

Fig. 3. ERp57-GFP translocates to the nucleus upon TNF-α treatment. HepG2 cells transiently transfected with ERp57-GFP were treated with vehicle (3 μl 0.1% BSA in PBS per 1,000 μl SF DMEM) or 30 ng/ml TNF-α in SF DMEM for 1 h or 15 min. The cells were stained for p65 (NF-κB, Red), and Draq5 nuclear stained (Blue, Nuclear). All are split channel images with the corresponding merge. A: One hour vehicle control treatment. B: Fifteen minutes TNF-α treatment. C: One hour TNF-α treatment. D: Fifteen minutes TNF-α treatment but p65 staining was blocked with a blocking peptide to show Ab specificity.

factor modification are topologically impossible if all of the protein resides in the ER. The proteosomal degradation pathway allows proteins to be retro-translocated from the ER to the cytosol [Hoseki et al., 2010], however, a molecular description of resident ER proteins escaping the secretory pathway to function properly in the cytosol or nucleus does not yet exist [Hoseki et al., 2010]. Alternatively, ERp57 may escape ER residency through its weak signal sequence, allowing for a cytoplasmic pool and separate function. This scenario would be analogous to calreticulin's inefficient compartmentalization due to its weak signal sequence, allowing regulation of glucocorticoid receptor-mediated gene activation [Shaffer et al., 2005]. In comparison to BiP, ERp57 has a destabilizing proline in the alpha helical portion of the signal sequence, possibly allowing different topological forms of ERp57. We determined through confocal microscopy that a majority of ERp57-GFP is strongly localized to the ER despite the destabilizing proline in the signal sequence. If this is due to a stronger than expected signal sequence, presence of translocon-associated stabilizing factors such as TRAM and TRAP, or a combination of the two mechanisms cannot be determined by these experiments. Some extra-ER structures did contain ERp57-GFP (Fig. 2A, white arrow) separate from ER-mRFP, but we cannot say if these round structures are lipid-derived vesicles, another organelle, or an artifact that should be examined further. Because the ER in HepG2 cells occupies a majority of cellular space, any potential ERp57-GFP signal outside of the ER is obscured by the intense ER expression.

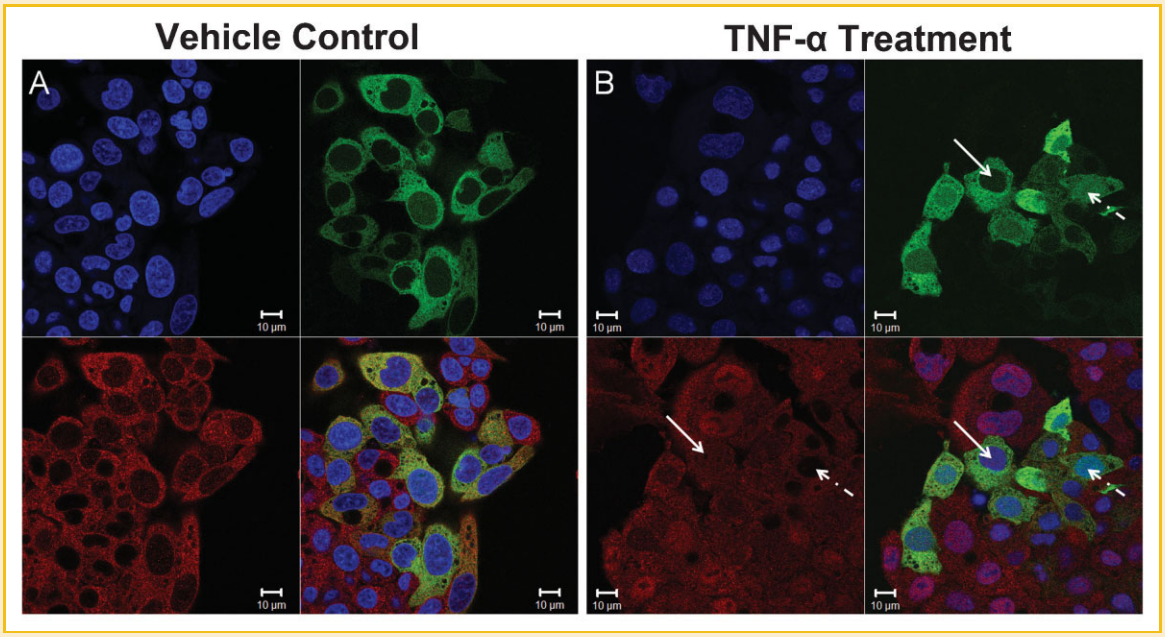

Fig. 4. TNF-α enhances CytoERp57-GFP localization to the nucleus. HepG2 cells transfected with cytoERp57-GFP were treated with vehicle (3 μl 0.1% (w/v) BSA in PBS per 1,000 μl SF DMEM) or 30 ng/ml TNF-α for 15 min. The cells were fixed, permeabilized, stained for p65 (NF-κB, Red), and Draq5 nuclear stained (Blue, Nuclear). All are split channel images with the corresponding merge. A: Vehicle treatment does not trigger nuclear translocation of p65, but some basal cytoERp57-GFP nuclear localization is seen. B: TNF-α treatment for 15 min increases the both the nuclear translocation of p65 and cytoERp57-GFP. However, p65 can have nuclear localization without cytoERp57-GFP (solid white arrow), and cytoERp57-GFP can have nuclear localization without p65 (dashed white arrow).

Therefore, we performed additional experiments to detect ERp57 distribution in HepG2 cells using subcellular fractionation, with the results indicating that a small population of ERp57 exists in the cytosol of HepG2 cells. It is not clear if this fraction is large enough to alter cellular functions, especially with respect to translocating to the nucleus to modulate gene transcription. However, in a study evaluating cytoplasmic and nuclear ERp57, the protein in these locations was only detectable through co-IP and chromatin immunoprecipitation, both very sensitive [Eufemi et al., 2004]. Thus, identifying even a small fraction of ERp57 in the cytosol, indicates the cytoplasmic fraction may possess important regulatory effects in HepG2 cells.

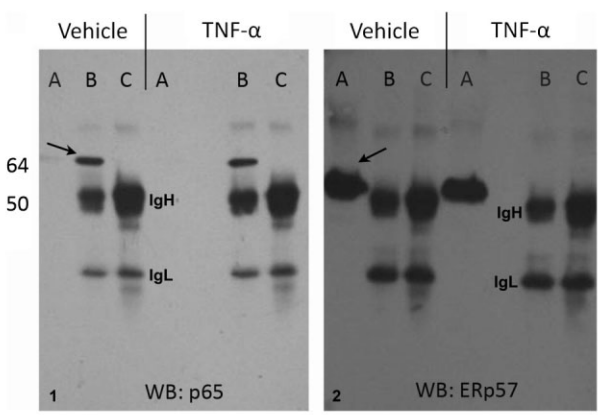

Fig. 5. NF-κB and ERp57 do not associate in HepG2 cells after TNF-α treatment by Co-IP. Cell cultures were treated either with BSA vehicle control or 30 ng/ml TNF-α for 15 min. The lysates were incubated either with p65 (NF-κB) or control IgG and Western blotted for p65 and ERp57. (A) Whole cell lysate (B) incubated with p65 Ab (C) incubated with control IgG. The arrows indicate the protein band for each Western blot.

ERp57-GFP DOES NOT TRANSLOCATE TO THE NUCLEUS UPON PMA AND 1,25(OH)$_2$D$_3$ TREATMENT IN HepG2 CELLS

Our attempts to induce nuclear localization of ERp57-GFP with PMA and 1,25(OH)$_2$D$_3$ treatments failed to show this occurs in HepG2 cells. This finding differs from those previously reported in several other cells types [Rohe et al., 2005; Wu et al., 2010]. Similar treatments triggered nuclear localization of ERp57 in neuromyeloid precursor cells [Wu et al., 2010]. Nuclear localization of ERp57 in rat intestinal IEC6 cells occurred after only a 5 min treatment with 1,25(OH)2D3 [Rohe et al., 2005]. Differences in cell-specific responses may be due to differences in cellular machinery among epithelia, hepatocytes, and hematopoietic cells, or may be related to alterations during transformation to a cancerous phenotype. Plasma membrane localization of ERp57 may be required for proper responses to 1,25(OH)$_2$D$_3$ and PKC activators, and plasma membrane localization has yet to be adequately explored in primary liver or HCC cells. However, confocal images from this study did not indicate strong cell surface membrane expression. Nevertheless, this result cannot exclude the possibility that the treatment times, concentrations, or combinations needed to trigger translocation of ERp57 to the nucleus in HepG2 cells.

IMPLICATIONS OF ERp57-GFP AND cytoERp57 TRANSLOCATION TO THE NUCLEUS UPON TNF-α TREATMENT

While TNF-α treatment triggered nuclear localization of ERp57-GFP in many cells on a relatively short timescale (15 min), it was not clear why cells adjacent to each other sometimes failed to respond similarly in otherwise identical treatments. Considering these HepG2 cells are not synchronized, ERp57 nuclear translocation may depend upon a certain stage of the cell cycle. Alternatively, it may be due to phenotypic microheterogeneity in the cell line. HepG2 transfectants expressing a cytoplasmic form of ERp57, cytoERp57-GFP, were developed as a proof-of-principle that cytoplasmic ERp57 can be produced in the cytosol and, when there, translocate into the nucleus. Results shown in Figure 4 demonstrated that cytoERp57-GFP indeed was expressed stably in the cytosol where it was able to translocate into the nucleus in response to treatment with TNF-α. This indicates that ERp57 expressed in HCC cells has a functioning NLS as has been predicted [Bourdi et al., 1995] and shown in other cells [Adikesavan et al., 2008]. Given that TNF-α has shown differential effects on HCC carcinogenesis and progression [Pikarsky et al., 2004], it is conceivable that ERp57 may contribute to this process.

ERp57 AND p65 OF NF-κB DO NOT DEPEND ON EACH OTHER FOR NUCLEAR TRANSLOCATION IN HepG2 CELLS

Results from both the co-IP experiments and confocal images after TNF-α treatment clearly indicate that ERp57 and the p65 subunit of the NF-κB heterodimer do not associate in HepG2 cells and neither do they depend on each other to translocate into the nucleus. As seen in Figure 4, TNF-α treatments demonstrated that p65 could move into the nucleus entirely independently of cytoERp57-GFP and vice versa. Furthermore, no evidence of strong co-localization of ERp57 and p65 was ever seen in HepG2 nuclei as yellow fluorescence. The co-IP experiments provide further support for this observation in Figure 5. Despite attempting several different variations, including stabilizing labile disulfide bonds with NEM, ERp57 was not observed in the p65 Ab incubated lysate nor p65 in the ERp57 Ab incubated lysate. Therefore, ERp57 and the p65 subunit of NF-κB do not appear to associate with each other to translocate into the nucleus of HepG2 cells even though both are stimulated to move by TNF-α. We cannot, however, preclude the possibility that ERp57 may associate with other NF-κB subunits. ERp57 has two conserved rel-homology binding domains for binding rel proteins, so it is plausible for this to occur [Khanal and Nemere, 2007].

In summary, we demonstrated that cytoplasmic ERp57 undergoes dynamic changes in HepG2 cellular localization after short exposure to TNF-α. Specifically, HepG2 cells treated for 15 min with 30 ng/ml TNF-α showed marked nuclear translocation of the cytoplasmic pool of ERp57-GFP. Unlike results with other cell types, PKC activation and $1,25(OH)_2D_3$ exposure produced no noticeable effects on ERp57-GFP in HCC cells. Subcellular fractionation and confocal microscopy revealed a small population of ERp57 in the cytosol. To verify this population of ERp57 can translocate to the nucleus, HepG2 cells were transfected with cytoERp57-GFP. This pool of ERp57 translocated to the nucleus upon TNF-α treatment, suggesting its NLS was active and the protein is properly folded in the cytosol. Additionally, the NF-κB subunit p65 failed to associate with ERp57 after TNF-α treatment, as evidenced by both co-IP experiments and confocal imaging, indicating their nuclear translocations occur independently in HepG2 cells. These studies shed light on the function and mobility of the cytoplasmic pool of ERp57 in HCC cells, and indicate that conditions that favor cytoplasmic localization are likely to increase nuclear localization and regulation of gene expression.

ACKNOWLEDGMENTS

This work was initiated by support from the Center for Translational Cancer Research and the Helen F. Graham Cancer Center in Newark, DE. The authors extend their thanks to JoAnne Julian, Dr. Kirk Czymmek, Dr. Ilka Nemere, and Dr. Kelly A. Meckling their many helpful discussions and ideas for this work. A special thanks goes to Dr. Erik Snapp for his advice, creativity and for providing the plasmids without which this work would not have been possible. BJG would like to acknowledge the scholarship support he received from the Howard Hughes Medical Institute and the Goldwater Foundation.

REFERENCES

Adikesavan AK, Unni E, Jaiswal AK. 2008. Overlapping signal sequences control nuclear localization and endoplasmic reticulum retention of GRP58. Biochem Biophys Res Commun 377:407–412.

Bourdi M, Demady D, Martin JL, Jabbour SK, Martin BM, George JW, Pohl LR. 1995. cDNA cloning and baculovirus expression of the human liver endoplasmic reticulum P58: Characterization as a protein disulfide isomerase isoform, but not as a protease or a carnitine acyltransferase. Arch Biochem Biophys 323:397–403.

Chichiarelli S, Ferraro A, Altieri F, Eufemi M, Coppari S, Grillo C, Arcangeli V, Turano C. 2007. The stress protein ERp57/GRP58 binds specific DNA sequences in HeLa cells. J Cell Physiol 210:343–351.

Cicchillitti L, Della Corte A, Di Michele M, Donati MB, Rotilio D, Scambia G. 2010. Characterisation of a multimeric protein complex associated with ERp57 within the nucleus in paclitaxel-sensitive and -resistant epithelial ovarian cancer cells: The involvement of specific conformational states of beta-actin. Int J Oncol 37:445–454.

Coppari S, Altieri F, Ferraro A, Chichiarelli S, Eufemi M, Turano C. 2002. Nuclear localization and DNA interaction of protein disulfide isomerase ERp57 in mammalian cells. J Cell Biochem 85:325–333.

El-Serag HB, Rudolph KL. 2007. Hepatocellular carcinoma: Epidemiology and molecular carcinogenesis. Gastroenterology 132:2557–2576.

El-Serag HB, Mason AC, Key C. 2001. Trends in survival of patients with hepatocellular carcinoma between 1977 and 1996 in the United States. Hepatology 33:62–65.

Eufemi M, Coppari S, Altieri F, Grillo C, Ferraro A, Turano C. 2004. ERp57 is present in STAT3-DNA complexes. Biochem Biophys Res Commun 323: 1306–1312.

Ferraro A, Altieri F, Coppari S, Eufemi M, Chichiarelli S, Turano C. 1999. Binding of the protein disulfide isomerase isoform ERp60 to the nuclear matrix-associated regions of DNA. J Cell Biochem 72:528–539.

Grillo C, D'Ambrosio C, Scaloni A, Maceroni M, Merluzzi S, Turano C, Altieri F. 2006. Cooperative activity of Ref-1/APE and ERp57 in reductive activation of transcription factors. Free Radic Biol Med 41:1113–1123.

Guo GG, Patel K, Kumar V, Shah M, Fried VA, Etlinger JD, Sehgal PB. 2002. Association of the chaperone glucose-regulated protein 58 (GRP58/ER-60/ERp57) with Stat3 in cytosol and plasma membrane complexes. J Interferon Cytokine Res 22:555–563.

Hirano N, Shibasaki F, Sakai R, Tanaka T, Nishida J, Yazaki Y, Takenawa T, Hirai H. 1995. Molecular cloning of the human glucose-regulated protein

ERp57/GRP58, a thiol-dependent reductase. Identification of its secretory form and inducible expression by the oncogenic transformation. Eur J Biochem 234:336–342.

Hoseki J, Ushioda R, Nagata K. 2010. Mechanism and components of endoplasmic reticulum-associated degradation. J Biochem 147:19–25.

Khanal RC, Nemere I. 2007. The ERp57/GRp58/1,25D3-MARRS receptor: Multiple functional roles in diverse cell systems. Curr Med Chem 14:1087–1093.

Leys CM, Nomura S, LaFleur BJ, Ferrone S, Kaminishi M, Montgomery E, Goldenring JR. 2007. Expression and prognostic significance of prothymosin-alpha and ERp57 in human gastric cancer. Surgery 141:41–50.

McGlynn KA, Tarone RE, El-Serag HB. 2006. A comparison of trends in the incidence of hepatocellular carcinoma and intrahepatic cholangiocarcinoma in the United States. Cancer Epidemiol Biomarkers Prev 15:1198–1203.

Muhlenkamp CR, Gill SS. 1998. A glucose-regulated protein, GRP58, is down-regulated in C57B6 mouse liver after diethylhexyl phthalate exposure. Toxicol Appl Pharmacol 148:101–108.

Nemere I. 2005. The 1,25D3-MARRS protein: Contribution to steroid stimulated calcium uptake in chicks and rats. Steroids 70:455–457.

Oliver JD, Roderick HL, Llewellyn DH, High S. 1999. ERp57 functions as a subunit of specific complexes formed with the ER lectins calreticulin and calnexin. Mol Biol Cell 10:2573–2582.

Pikarsky E, Porat RM, Stein I, Abramovitch R, Amit S, Kasem S, Gutkovich-Pyest E, Urieli-Shoval S, Galun E, Ben-Neriah Y. 2004. NF-kappaB functions as a tumour promoter in inflammation-associated cancer. Nature 431:461–466.

Rohe B, Safford SE, Nemere I, Farach-Carson MC. 2005. Identification and characterization of 1,25D3-membrane-associated rapid response, steroid (1,25D3-MARRS)-binding protein in rat IEC-6cells. Steroids 70: 458–463.

Seliger B, Stoehr R, Handke D, Mueller A, Ferrone S, Wullich B, Tannapfel A, Hofstaedter F, Hartmann A. 2009. Association of HLA class I antigen abnormalities with disease progression and early recurrence in prostate cancer. Cancer Immunol Immunother 59:529–540.

Shaffer KL, Sharma A, Snapp EL, Hegde RS. 2005. Regulation of protein compartmentalization expands the diversity of protein function. Dev Cell 9:545–554.

Tourkova IL, Shurin GV, Chatta GS, Perez L, Finke J, Whiteside TL, Ferrone S, Shurin MR. 2005. Restoration by IL-15 of MHC class I antigen-processing machinery in human dendritic cells inhibited by tumor-derived gangliosides. J Immunol 175:3045–3052.

Wu W, Beilhartz G, Roy Y, Richard CL, Curtin M, Brown L, Cadieux D, Coppolino M, Farach-Carson MC, Nemere I, Meckling KA. 2010. Nuclear translocation of the 1,25D(3)-MARRS (membrane associated rapid response to steroids) receptor protein and NFkappaB in differentiating NB4 leukemia cells. Exp Cell Res 316:1101–1108.

Zhou WM, Ping JL, Qian FC, Zhang GL. 2009. Expression characteristics of nuclear factor kappa B in hepatocellular carcinoma tissues. Zhonghua Gan Zang Bing Za Zhi 17:843–846.